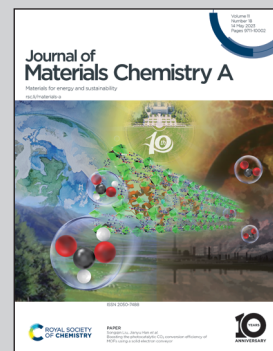


Showcasing research from Los Alamos National Laboratory, New Mexico.

Fluoroalkyl phosphonic acid radical scavengers for proton exchange membrane fuel cells

Radical attack on perfluorosulfonic acid membranes is detrimental to the long-term durability of proton-exchange membrane fuel cells. The radical scavenging efficiency of state-of-the-art cerium antioxidants is limited by their high mobility. Here, we found that fluoroalkyl phosphonic acids can surpass the radical scavenging activity of cerium without the migration issue. Computational studies confirm the radical scavenging mechanism of fluoroalkyl phosphonic acids in an acidic environment. This study implies that fluoroalkyl phosphonic acid incorporation can improve fuel cell durability for heavy-duty applications.

As featured in:



See Yu Seung Kim, Rod Borup et al., *J. Mater. Chem. A*, 2023, **11**, 9748.



Cite this: *J. Mater. Chem. A*, 2023, **11**, 9748

Received 5th December 2022
Accepted 6th April 2023

DOI: 10.1039/d2ta09421e

rsc.li/materials-a

Radical-induced degradation of proton exchange membranes limits the durability of proton-exchange membrane fuel cells. Cerium is widely used as a radical scavenger, but the migration of cerium ions to the catalyst layer has been an unresolved issue, reducing its effectiveness over time. Here, we report phosphonic acids as a promising class of radical scavengers, showing competent radical scavenging activity compared to cerium without the migration issue. The *ex situ* Fenton test shows that the fluoride emission rate for Nafion membrane incorporated with fluoroalkyl phosphonic acid ranged from 0.22 to 0.37 $\mu\text{g F cm}^{-2} \text{ h}^{-1}$, lower than that of the cerium-incorporated NafionTM membrane (0.39 $\mu\text{g F cm}^{-2} \text{ h}^{-1}$). The *in situ* open circuit voltage hold test confirmed that a phosphonic acid-incorporated NafionTM membrane has a 58% lower fluoride emission rate compared to the baseline. Density functional theory calculations indicate that the activation energy of the hydroxyl radical scavenging reaction of an alkyl phosphonic acid is only 0.68 eV, suggesting an effective radical scavenging pathway.

Proton exchange membranes (PEMs) transport protons while preventing the diffusion of hydrogen and oxygen between the anode and cathode electrodes. However, the small amounts of gases that cross over through the PEM cause the generation of hydrogen peroxide at the catalyst layers. This peroxide breaks down into radicals that degrade PEMs, leading to the eventual failure of the fuel cell devices.¹ The prominent sites for the attack in perfluorosulfonic acid (PFSA) membranes like that

Fluoroalkyl phosphonic acid radical scavengers for proton exchange membrane fuel cells†

Tanya Agarwal, ^{ae} Santosh Adhikari, ^a Yu Seung Kim, ^{*a} Siddharth Komini Babu, ^a Ding Tian, ^b Chulsung Bae, ^b Nguyet N. T. Pham, ^c Seung Geol Lee, ^d Ajay K. Prasad, ^e Suresh G. Advani, ^e Allen Sievert, ^f Wipula Priya Rasika Liyanage, ^a Timothy E. Hopkins, ^f Andrew Park ^f and Rod Borup ^{*a}

discussed in this paper include the terminal carboxylic acid groups, ether groups in the side chains, tertiary carbon atoms, and the sulfonic acid C-S bonds.^{2,3} Usually, a radical attack causes the polymer chain to fragment, referred to as the unzipping reaction. Unreacted carboxylic groups in PFSA react with hydroxyl radicals forming CO₂ and HF. This causes the formation of the terminal CF₂ unit. This unzipping proceeds ultimately reaching a side chain which causes loss of the overall side chain.

Attack on the side chain C-S is one of the most important mechanisms of PFSA degradation. Attack of hydroxyl radicals on the terminal $R_F\text{-CF}_3\text{-SO}_3\text{H}$ results in the formation of the $R_F\text{-CF}_2$ radical. This terminal radical then reacts with the hydroxyl radical forming $R_F\text{-CF}_2\text{-OH}$. $R_F\text{-CF}_2\text{-OH}$ reacts with water and results in the subsequent release of HF which causes the formation of -COOH acid groups. Attack on the ether bonds close to the sulfonic acid is perhaps the dominant mechanism of side chain degradation followed by the attack on the tertiary carbon atoms. Attack on the ether bond results in the formation of side group $R_F\text{-CF}_2\text{-O}$ radicals which react with water causing HF release and carboxylic acid end group. This further unzips the PFSA chain by the mechanism discussed above.

Cerium is widely used as a radical scavenger because of its ability to switch rapidly between oxidation states. Cerium below 0.6 wt% in the PEM reduces voltage degradation by a factor of 20 while reducing the fluoride emission rate (FER) by orders of magnitude over non-modified NafionTM.^{4,5} Because of the highly efficient radical scavenging activity, Toyota Motors implemented the cerium technology into their MIRAI fuel cell vehicles to improve fuel cell durability. Although they are effective radical scavengers, cerium ions tend to migrate through the PEM under fuel cell operating conditions,^{6,7} which reduces the radical scavenging activity over time,⁸ depriving the PEM of the benefits of cerium incorporation.⁹ There are several approaches to stabilizing cerium in the membrane. Zirconium doping reduces the dissolution rate of cerium oxide to enhance cerium stability.^{10,11} Graphene oxides¹² and carbon nanotubes^{13,14} have been used for the durability enhancement of membranes

^aMAP-11: Materials Synthesis & Integrated Devices, Los Alamos National Laboratory, Los Alamos, NM 87545, USA. E-mail: yskim@lanl.gov; borup@lanl.gov

^bDepartment of Chemistry and Chemical Biology, Rensselaer Polytechnic Institute, Troy, NY 12180, USA

^cUniversity of Science, Vietnam National University, Ho Chi Minh City, Viet Nam

^dSchool of Chemical Engineering, Pusan National University, Busan, 46241, Republic of Korea

^eCenter for Fuel Cells and Batteries, Department of Mechanical Engineering, University of Delaware, Newark, DE 19716, USA

^fThe Chemours Company FC, LLC, Wilmington, DE 19899, USA

† Electronic supplementary information (ESI) available. See DOI: <https://doi.org/10.1039/d2ta09421e>



incorporated with cerium. However, the additional material incorporation can cause other issues, such as mechanical property deterioration, conductivity loss, FER reduction, and processing complexity.

Several organic radical scavengers based on phenolic and quinone derivatives have been considered for stabilizing PEMs. α -Tocopherol, hydroquinone, 2,2-bipyridine, and 2,6-dimethoxy-1,4-benzoquinone are investigated as radical scavengers for sulfonated poly(arylene ether sulfone).¹⁵ Quercetin was investigated as the radical scavenger for NafionTM and found to double the durability of the membrane.¹⁶ Ferrocyanide,¹⁴ cinnamic acid,¹⁷ and terephthalic acid¹⁸ were tested as radical scavengers for NafionTM. Recently, Alizarin was investigated as a radical scavenger and was found to aid the cerium activity, surpassing the open circuit voltage (OCV) lifetime of 450 h.¹⁹ However, the radical scavenging activity of the organic radical scavengers investigated in the literature is low compared to that of cerium.^{15–17} Moreover, these chemistries also suffer from problems like poor dispersive ability and show limited flexibility of incorporation in the PFSA membrane.

Phosphorus compounds such as phosphoric acids, phosphates, phosphonates, and phosphonic acids are excellent antioxidants in fire extinguishers and biological industries.²⁰ Phosphorus compounds are also known for their exceptional stability under potential conditions of fuel cells over thousands of operating hours.²¹ However, to the best of our knowledge, phosphorus compounds are not investigated as radical scavengers in fuel cells or other electrochemical devices. Here, we report fluoroalkyl phosphonic acids as effective radical

scavengers for PEMs using *ex situ* Fenton's testing and *in situ* OCV hold accelerated stress tests (ASTs). We show the impact of phosphonic acid radical scavengers on the properties of the membranes and investigate the migration issue. We then discuss the radical scavenging mechanisms of phosphonic acids that might explain our findings.

Fig. 1a compares the FER of the non-modified NafionTM (Baseline), cerium-incorporated NafionTM (Ce) at a loading of 5 mol%, and fluoroalkyl phosphonic acid-incorporated NafionTM at a loading of 30 mol% in aqueous Fenton (*ex situ*) tests. The FER of the Baseline measured with the Fenton test was $0.85 \mu\text{F cm}^{-2} \text{h}^{-1}$, which is significantly higher than those of Ce ($0.39 \mu\text{F cm}^{-2} \text{h}^{-1}$) and phosphonic acid-NafionTM membranes ($0.22\text{--}0.37 \mu\text{F cm}^{-2} \text{h}^{-1}$). The decay of fluorescence intensity of 6-carboxyfluorescein dye in the presence of the Fenton reagent was monitored with and without radical scavengers to verify the high radical scavenging activity of phosphonic acids observed in the aqueous Fenton test (Fig. S1†). Fig. 1b shows the ratio of fluorescence intensity (I) after the addition of Fenton's reagent with and without scavengers to the fluorescence intensity of the un-degraded dye (I_0). The decay of the dye is suppressed significantly in the presence of phosphonic acids, with all phosphonic acids showing higher retention of the intensity of the fluorescent dye (I) compared to cerium. This result confirms the fact that phosphonic acids indeed have higher radical scavenging capability compared to cerium in the presence of transition metal ions.

The radical scavenging activity of the phosphonic acids depends on the fluoroalkyl chain length. The highest radical

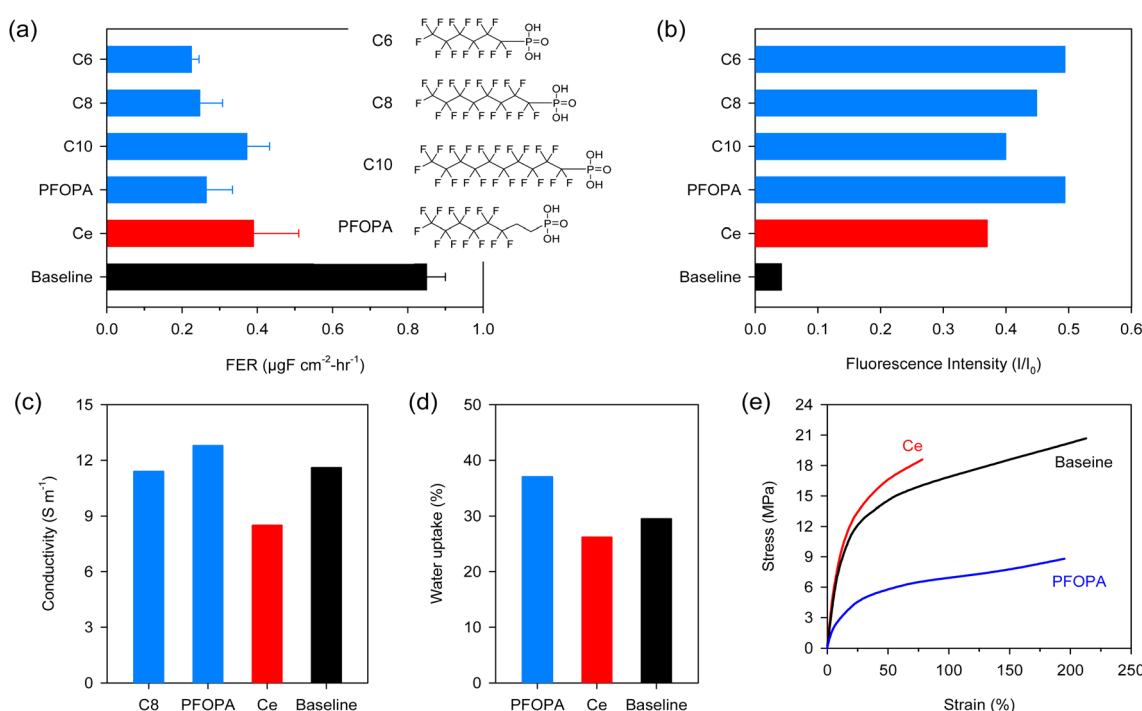


Fig. 1 Properties of radical scavenger-incorporated NafionTM membranes: (a) FER over 24 hours of aqueous Fenton test, (b) retention of 6-carboxyfluorescein intensity in the presence of various radical scavengers, (c) proton conductivity at 80 °C and 100% RH, (d) water uptake at room temperature, and (e) stress–strain curves under ambient conditions.



scavenging activity was obtained with the shortest perfluoro chains (C6) and decreased with increasing the chain length. The lower radical scavenging activity of the longer phosphonic acids may be due to the dilution with non-reactive perfluoro chains. Partially fluorinated phosphonic acid with eight carbon long chain length (PFOPA, $pK_a = 2.3$) has similar radical scavenging activity to C6 and C8 ($pK_a = 1.85$). The insignificant effect of the pK_a of the phosphonic acids on radical scavenging activity is in stark contrast with the use of phosphonic acid as an immobilizer for cerium where higher cerium retention was obtained with a phosphonic acid with higher pK_a .²²

While phosphonic acids show promising radical scavenging activity, it is crucial that the compromise on the other desirable properties of NafionTM, such as conductivity and mechanical strength, should be minimal. PFOPA enhanced the conductivity of NafionTM by 10%, while comparable conductivity was observed for the C8 incorporated membrane (Fig. 1c). Since phosphonic acids are proton conductors, enhanced conductivity is not surprising. Higher conductivity with the PFOPA-NafionTM over the C8-NafionTM may be due to the higher hydrophilicity of PFOPA, facilitating structural diffusion of protons. The cerium incorporated NafionTM exhibited reduced conductivity because cerium makes a fraction of sulfonic acid

sites (based on loading) unavailable for proton conduction leading to a cross-linking effect.¹¹ The PFOPA-incorporated NafionTM membrane showed higher water uptake (Fig. 1d). This corroborated with the higher conductivity observed for these membranes.

Mechanical properties affect chemical durability and are therefore critical to investigate.²² Incorporating cerium into NafionTM makes the membrane brittle, *i.e.*, with a higher modulus but lower elongation (Fig. 1e). Incorporating PFOPA decreases the modulus while maintaining elongation. The strength of the PFOPA-incorporated NafionTM is low, but the elongation at break is slightly lower than the Baseline. As a result, the tensile toughness of the cerium (5 mol%) and PFOPA (30 mol%)-incorporated NafionTM membranes is comparable (Fig. S2†). The mechanical properties of the PFOPA-incorporated membranes are a function of the content of the phosphonic acid in the composite membrane (Fig. S3†). It appears that phosphonic acids have a plasticizing effect on the membrane with strength and modulus decreasing and elongation increasing with higher loadings of phosphonic acid.

To assess the migration resistance of radical scavengers, we examined the distribution of the cerium and phosphonic acids in NafionTM by energy-dispersive X-ray spectroscopy (EDX) after the

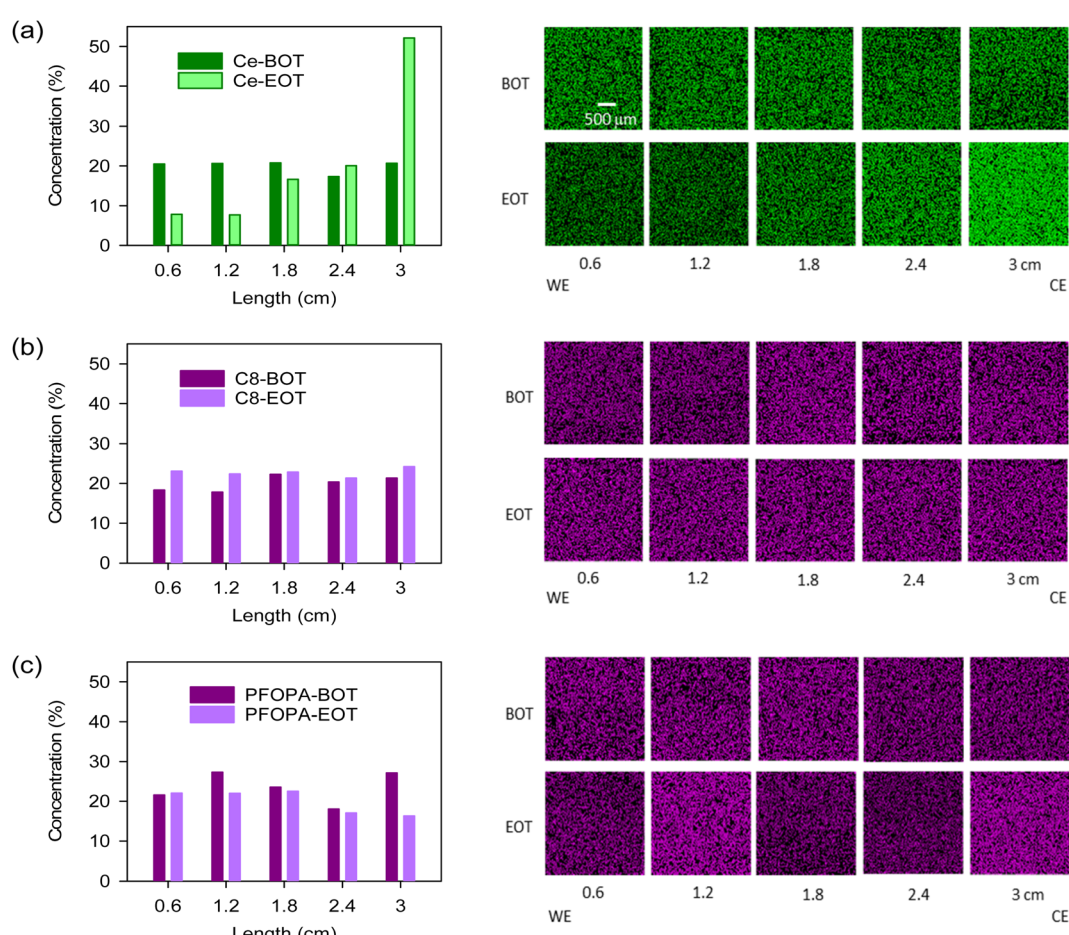


Fig. 2 Distribution of radical scavengers in the NafionTM membrane after the hydrogen pump experiment conducted at a 0.4 V potential gradient till 2C charge transfer: (a) Ce-NafionTM, (b) C8-NafionTM and (c) PFOPA-NafionTM. The counter electrode (CE) was located 3 cm from the working electrode (WE). EDX images were taken at the beginning of the test (BOT) and end of the test (EOT).



samples were subjected to a 0.4 V potential gradient till a total of 2C charge transfer was achieved. This *ex situ* test well simulates the *in situ* migration of cerium during fuel cell operation.²³ For the Ce-Nafion™ membrane, the concentration of cerium drastically increased toward the counter electrode (CE) after the migration test (Fig. 2a). The migration of cerium under potential conditions is also evident from the X-ray fluorescence (XRF) line scan (Fig. S4†), where the concentration of cerium towards the counter electrode is approximately 3 times higher than that in the part toward the working electrode (WE) at the end of the test. As opposed to cerium, C8 and PFOPA showed uniform distribution before and after the test (Fig. 2b and c). Slight redistribution occurred likely due to an initial non-uniform distribution of phosphonic acid in the as-cast membrane. This could also be due to the relatively high swelling for these membranes and the non-flat nature of the membrane when performing EDX analysis. This test was designed to study the migration of radical scavengers driven by potential gradients and mobility under high humidities and temperatures. Therefore, the minimal migration of phosphonic acids does not mean that they are resistant to migration under all conditions, such as pressure gradients and water fluxes. Nevertheless, the test shows the increased resistance of these non-water-soluble radical scavengers to migration when compared to cerium.

After validating the radical scavenging activity and migration resistance of the phosphonic acids, we examined the *in situ* performance of the PFOPA-incorporated Nafion™ using the US Department of Energy (DOE) protocols. The H₂/air fuel cell performance was measured with 5 cm² differential cells after conditioning the membranes in humidified conditions over two days. The performance of the cell using the PFOPA-incorporated

membrane was lower than that of the cell using the Baseline and Ce-Nafion™ membranes (Fig. 3a). High-frequency resistance (HFR) is similar for all three membranes ($\sim 0.054 \Omega \text{ cm}^2$) (Fig. S5†). Cyclic voltammogram (CV) data suggests that the active sites on Pt(100) were reduced for the cell using the PFOPA-incorporated membrane (Fig. 3b), causing the lower performance of the PFOPA cell.²⁴ It is also to be noted that the capacitance for the PFOPA cell is lower. The observations from CV data are supported by the high Tafel slope and lower mass activity for the cell using the PFOPA-incorporated Nafion™ (Fig. 3c). This result indicates that phosphonic acid leaching from the membrane can affect catalyst activity, although the impact on overall performance is not substantial. It is to be noted that our conditioning protocol incorporates break-in of the cell under flooded conditions for large periods of time. This situation can aggravate the migration of immobile species. This is not the situation we simulated in the migration test and is unlikely to be experienced in an operating fuel cell.

Next, we validated the radical scavenging activity of phosphonic acids using the US DOE membrane durability AST protocol which consists of holding the fuel cell at 90 °C at 30% RH under OCV conditions.²⁵ The Baseline cell started to fail after 175 hours in the OCV hold test, but the cells using Ce-Nafion™ and PFOPA-Nafion™ were stable for more than 200 hours without signs of failure evident (Fig. 3d). The initial H₂ crossover current density of the MEAs using Ce-Nafion™ and PFOPA-Nafion™ was $\sim 5 \text{ mA cm}^{-2}$, notably higher than that using the baseline MEA ($\sim 1.75 \text{ mA cm}^{-2}$) (Fig. 3e). The higher crossover for the PFOPA membrane could be due to the higher water uptake, unoptimized fabrication process of the MEAs and non-uniformities in the membrane casting process. Fig. 3f

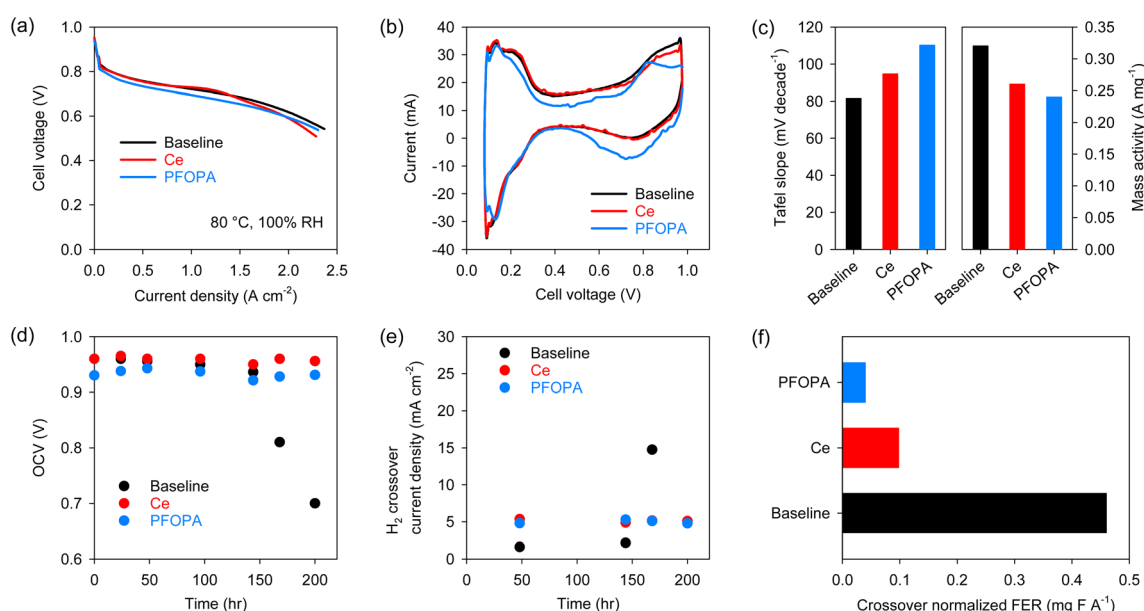


Fig. 3 *In situ* performance of radical scavenger incorporating MEAs: (a) *iR*-corrected polarization curves of the MEAs under H₂/air, at flow rates of 1000 and 3000 sccm on the anode and cathode, respectively, (b) CVs of the MEAs for the Ce and PFOPA incorporating membranes, (c) Tafel slope and mass activity at 0.9 V under H₂/air conditions, (d) OCV and (e) H₂ crossover current density for the MEAs for the Ce and PFOPA incorporating membranes during the chemical durability test, and (f) crossover normalized FER for the MEAs using the Ce and PFOPA incorporating membranes during the chemical durability test.



shows the H_2 crossover normalized FER calculated from the non-normalized total FER emissions during the stable OCV operation of different membranes. The H_2 crossover normalized FER of the PFOPA-NafionTM membrane was 0.04 mg F A⁻¹, which is 58% lower than that of the Ce-NafionTM membrane for the same duration, confirming the stronger radical scavenging activity of phosphonic acids compared to cerium. Even with

a higher crossover, the total FER for the PFOPA membrane is lower than for the Ce membrane (Fig. S6†). The FER trend from Fenton's test and OCV hold test differ considerably, corroborating the long-held belief that Fenton's test may not be an accurate predictor for membrane degradation under fuel cell operating conditions.

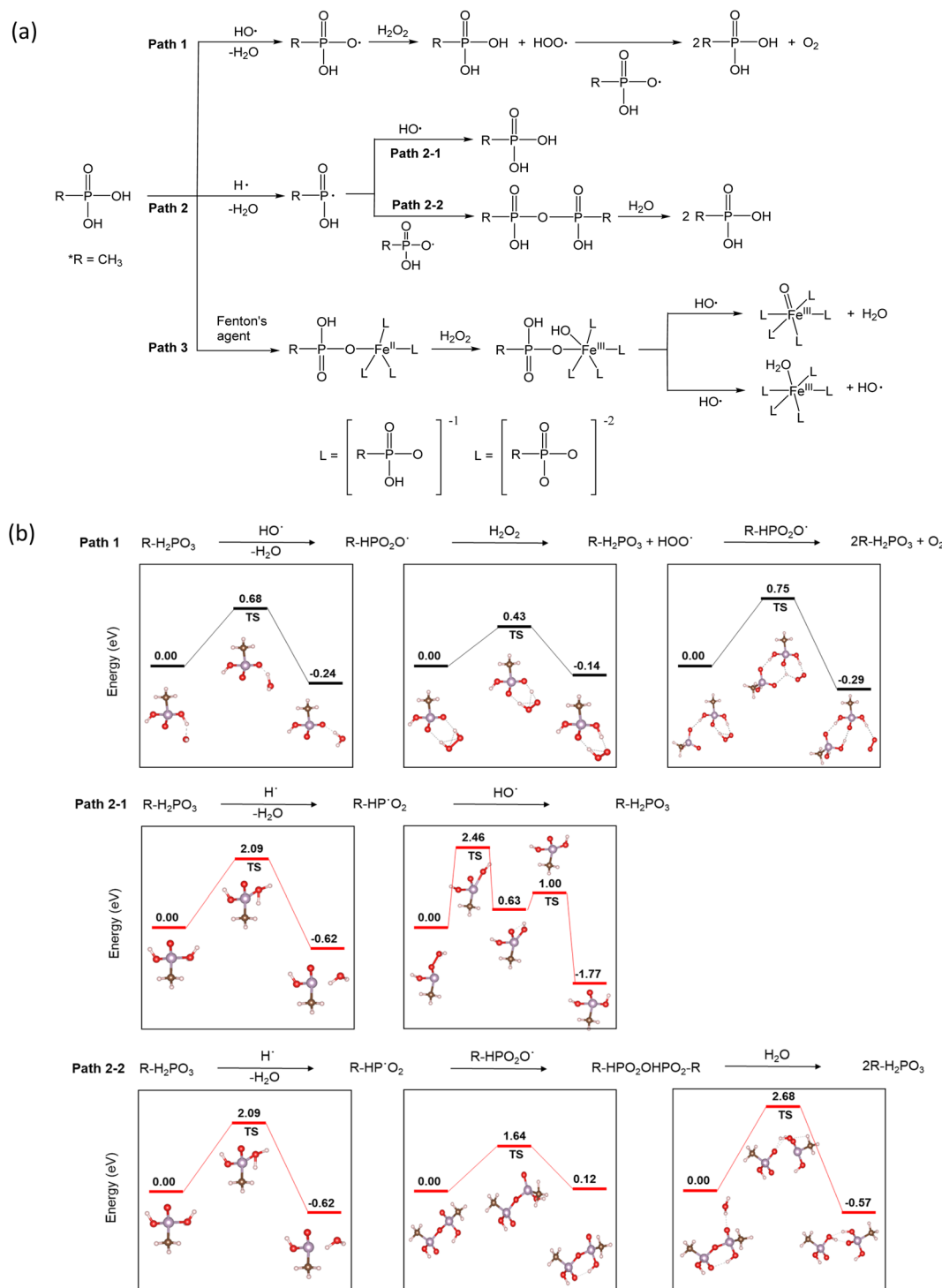


Fig. 4 Proposed radical scavenging mechanisms of phosphonic acids: (a) three reaction pathways, (b) reaction activation energy of Path 1 and Path 2.



The use of phosphonic acids in fuel cell systems for radical scavenging is intriguing, and so is the mechanism of their action. In accordance with the density functional theory (DFT) investigation of reaction pathways for phosphoric acid in the presence of different radicals,²⁶ three pathways are possible (Fig. 4a). Under fuel cell operating conditions, the radical species HO[·], H[·], and HOO[·] have been detected in the MEAs. The hydroxyl radical is the most aggressive intermediate. Primary sources of the hydroxyl radical (HO[·]) are slow homolysis of H₂O₂ (H₂O₂ → 2HO[·]) and the Fenton reaction (Fe²⁺ + H₂O₂[·] + H⁺ → Fe³⁺ + HO[·] + H₂O). The hydroxyl radicals can react with phosphonic acids to produce phosphonate radicals²⁶ (Path 1). The DFT calculations based on the Vienna *ab initio* simulation package (VASP)^{27,28} indicate that the activation energy of Path 1 is low (0.65 eV) (Fig. 4b). Hydrogen radicals (H[·]) are also generated through the reaction of HO[·] with H₂ (HO[·] + H₂ → H[·] + H₂O). Most of the HO[·] reacts with H₂ to form H[·], which then rapidly reacts with O₂ to form HOO[·] under fuel cell operating conditions.²⁹ P-centered radicals can react with hydroxyl radicals regenerating phosphonic acid (Path 2-1).³⁰ Alternatively, the P-centered radicals can combine to make phosphonic acid anhydride³¹ (Path 2-2). The reaction activation energy for Path 2-1 (2.46 eV) is slightly lower than that for Path 2-2 (2.68 eV). However, the activation energy for Path 2 is much higher than that for Path 1, suggesting that the radical scavenging action with phosphonic acids predominantly occurs with Path 1.

Under the Fenton test conditions, phosphonic acid can chelate with metal ions such as Fe²⁺ and affect the catalytic activity of Fe towards radical formation (Path 3). Yoshimura *et al.*³² observed a decrease in lipid peroxidation in Fenton's solution in the presence of phosphate buffer due to a decrease in ·OH radical formation. The spin-trapping experiments showed much reduced radical formation in phosphate buffer.³³ From the DFT calculations,³³ it looks like Path 3 might be a plausible reaction pathway for phosphonic acid in the presence of transition metal ions. The reaction activation energy for Path 3 is relatively low (~0.6 eV). The highly active radical scavenging activity of alkyl phosphonic acids is consistent with our results that show a lower FER of the phosphonic acid-incorporated NafionTM under *ex situ* (with Fe²⁺) and *in situ* (without Fe²⁺) conditions. From the calculations, it appears that when transition metals are present, Path 3 is the dominant pathway while Path 1 is the dominant mechanism for radical scavenging in the presence of hydroxyl radicals only. Path 2 is less likely to contribute to the durability enhancement observed in this study.

Conclusions and outlook

Our results show that phosphonic acids are promising radical scavengers for overcoming the challenges associated with lanthanide and other metal oxide-based radical scavenging systems.³⁴ Chain length, molecular weight, and aromaticity might influence the radical scavenging activity of phosphonic acids. To be effective radical scavengers, phosphonic acids should be non-water soluble. Tethering phosphonic acids into polymeric materials may be desirable for enhancing stability.³⁵ The dependence

of phosphonic acid concentration on the radical scavenging efficacy and the impact on membrane properties is currently being investigated. The influence of various metal ions in the system on the radical scavenging properties of phosphonic acids is of interest, particularly for the fuel cell systems using Pt-alloy-based catalysts or Pt group metal-free catalysts as phosphonic acids can chelate with metal ions such as Fe and Co. This can indirectly contribute to the chemical durability enhancement by trapping these peroxide decomposition catalysts. The radical scavenging activity of phosphonic acids under less acidic environments such as sulfonated or quaternized hydrocarbon membranes might be different and needs further study.

Author contributions

Tanya Agarwal: conceptualization, methodology, investigation, writing – original draft. Santosh Adhikari: writing – original draft, investigation, formal analysis. Yu Seung Kim: conceptualization, supervision, writing – original draft, writing – review & editing. Siddharth Komini Babu: methodology, investigation, supervision. Ding Tian: investigation. Chulsung Bae: methodology, supervision. Nguyet N. T. Pham: formal analysis, investigation. Seung Geol Lee: methodology, investigation, supervision. Ajay K. Prasad: methodology, supervision, writing – review & editing. Suresh G. Advani: methodology, supervision. Allen Sievert: formal analysis, investigation. Timothy Hopkins: formal analysis, investigation. Andrew Park: methodology, formal analysis, investigation. Rod Borup: writing – review & editing, supervision, funding acquisition.

Conflicts of interest

T. A., S. A., S. K. B., Y. S. K., R. B., A. K. P., and S. G. A. filed a US patent application in October 2022, U.S. Serial No. 63/422,732, related to the fluoroalkyl phosphonic acid-incorporated membrane composition in this article. A. S., T. H., and A. P. are employed by The Chemours Company FC, LLC. The remaining authors declare no competing interests.

Acknowledgements

The US Department of Energy (US DOE), Office of Energy Efficiency and Renewable Energy (EERE), and Hydrogen and Fuel Cell Technologies office (HFTO) supported this research through the M2FCT (Million Mile Fuel Cell Truck) Consortium.

References

- 1 T. H. Yu, Y. Sha, W. G. Liu, B. V. Merinov, P. Shirvaniyan and W. A. Goddard, *J. Am. Chem. Soc.*, 2011, **133**, 19857–19863.
- 2 M. Zaton, J. Roziere and D. J. Jones, *Sustainable Energy Fuels*, 2017, **1**, 409–438.
- 3 Z. Rui and J. Liu, *Prog. Nat. Sci.: Mater. Int.*, 2020, **30**, 732–742.
- 4 P. Trogadas, J. Parrondo and V. Ramani, *Electrochem. Solid-State*, 2008, **11**, B113–B116.



5 F. D. Coms, H. Liu and J. E. Owejan, *ECS Trans.*, 2008, **16**, 1735–1747.

6 A. M. Baker, S. Komini Babu, R. Mukundan, S. G. Advani, A. K. Prasad, D. Spernjak and R. L. Borup, *J. Electrochem. Soc.*, 2017, **164**, F1272–F1278.

7 H. Matsui, S. Takao, K. Higashi, T. Kaneko, G. Samjeske, T. Uruga, M. Tada and Y. Iwasawa, *ACS Appl. Mater. Interfaces*, 2022, **14**, 6762–6776.

8 S. M. Stewart, D. Spernjak, R. Borup, A. Datye and F. Garzon, *ECS Electrochem. Lett.*, 2014, **3**, F19–F22.

9 K. H. Wong and E. Kjeang, *J. Electrochem. Soc.*, 2017, **164**, F1179–F1186.

10 A. M. Baker, S. T. D. Williams, R. Mukundan, D. Spernjak, S. G. Advani, A. K. Prasad and R. L. Borup, *J. Mater. Chem. A*, 2017, **5**, 15073–15079.

11 J. Choi, J. H. Yeon, S. H. Yook, S. Shin, J. Y. Kim, M. Choi and S. Jang, *ACS Appl. Mater. Interfaces*, 2021, **13**, 806–815.

12 D. C. Seo, I. Jeon, E. S. Jeong and J. Y. Jho, *Polymers*, 2020, **12**, 1375.

13 A. M. Baker, L. Wang, W. B. Johnson, A. K. Prasad and S. G. Advani, *J. Phys. Chem. C*, 2014, **118**, 26796–26802.

14 K. R. Yoon, J. M. Kim, K. A. Lee, C. K. Hwang, S. G. Akpe, Y. J. Lee, J. P. Singh, K. H. Chae, S. S. Jang, H. C. Ham and J. Y. Kim, *J. Power Sources*, 2021, **496**, 229798.

15 S. H. Shin, A. Kodir, D. Shin, S. H. Park and B. Bae, *Electrochim. Acta*, 2019, **298**, 901–909.

16 Z. Y. Rui, J. Y. Wang, J. Li, Y. F. Yao, Y. X. Huo, J. G. Liu and Z. G. Zou, *J. Electrochem. Soc.*, 2019, **166**, F3052–F3057.

17 Y. Park and D. Kim, *J. Membr. Sci.*, 2018, **566**, 1–7.

18 Y. Zhu, S. Pei, J. Tang, H. Li, L. Wang, W. Z. Yuan and Y. Zhang, *J. Membr. Sci.*, 2013, **432**, 66–72.

19 K. Xu, S. Pei, W. Zhang, Z. Han, G. Liu, X. Xu, J. Ma, Y. Zhang, F. Liu and Y. Zhang, *J. Membr. Sci.*, 2022, **655**, 120594.

20 O. L. Bouamrane, A. Hellal, K. Hachama, L. Touafri, I. Haddadi, H. Layaida, I. Kirouani, A. Hassani, M. Mersellem, A. Madani and C. Bensouici, *J. Mol. Struct.*, 2022, **1250**, 131714.

21 K. H. Lim, A. S. Lee, V. Atanasov, J. Kerres, S. Adhikari, S. Maurya, E. J. Park, L. D. Manriquez, J. Jung, C. Fujimoto, I. Matanovic, J. Jankovic, Z. Hu, H. Jia and Y. S. Kim, *Nat. Energy*, 2022, **7**, 248–259.

22 T. Agarwal, I. Matanovic, S. Adhikari, E. J. Park, S. Komini Babu, Y. S. Kim, D. Tian, C. Bae, O. Morales-Collazo, J. F. Brennecke, A. K. Prasad, S. G. Advani, A. Sievert, T. Hopkins, A. Park and R. Borup, *J. Power Sources*, 2022, **554**, 232320.

23 V. M. Ehlinger, A. Kusoglu and A. Z. Weber, *J. Electrochem. Soc.*, 2019, **166**, F3255–F3267.

24 E. Westsson, S. Picken and G. Koper, *Front. Chem.*, 2020, **8**, 163.

25 T. J. Schmidt, *ECS Trans.*, 2006, **1**, 19.

26 H. C. Li, M. Hua, X. H. Pan, S. C. Li, X. X. Guo, H. Zhang and J. C. Jiang, *J. Mol. Model.*, 2019, **25**, 255.

27 G. Kresse and J. Furthmüller, *Comput. Mater. Sci.*, 1996, **6**, 15–50.

28 G. Kresse and J. Furthmüller, *Phys. Rev. B: Condens. Matter Mater. Phys.*, 1996, **54**, 11169.

29 M. Danilczuk, F. D. Coms and S. Schlick, *J. Phys. Chem. B*, 2009, **113**, 8031–8042.

30 L. Gubler, S. M. Dockheer and W. H. Koppenol, *ECS Trans.*, 2011, **41**(11), 1431–1439.

31 C. C. Xia, H. H. Geng, X. B. Li, Y. Y. Zhang, F. Wang, X. W. Tang, R. E. Blake, H. Li, S. J. Chang and C. Yu, *RSC Adv.*, 2019, **9**, 31325–31332.

32 Y. Yoshimura, Y. Matsuzaki, T. Watanabe, K. Uchiyama, K. Ohsawa and K. Imaeda, *J. Clin. Biochem. Nutr.*, 1992, **13**, 147–154.

33 H. Y. Chen, *ACS Omega*, 2019, **4**, 14105–14113.

34 T. Kwon, Y. Lim, J. Cho, R. Lawler, B. J. Min, W. A. Goddard III, S. S. Jang and J. Y. Kim, *Mater. Today*, 2022, **58**, 135–163.

35 J. Wang, Y. Dai, R. Y. Wan, W. Wei, S. C. Xu, F. H. Zhai and R. H. He, *Chem. Eng. J.*, 2021, **413**, 127541.

